[PS]Geochemical Modeling of the Near-Surface Hydrothermal System Beneath the Southern Moat of Long Valley Caldera, California*

Regina Tempel[1] and Daniel Sturmer[2]

[1]University of Nevada, Reno, Reno, NV (gtempel@unr.edu)
[2]University of Nevada, Reno, Reno, NV

Abstract

Geochemical reaction path and mass balance modeling techniques were used to test the hypothesis that an eastwardly flowing plume of thermal water in the southern moat of the Long Valley caldera system reacts with hydrothermally-altered intra-caldera tuffs and mixes with non-thermal groundwater. Our conceptual model was based on hypotheses in the literature and utilized published geochemical and petrologic data. Mixing of thermal and non-thermal waters and reaction with wall rock were simulated using the reaction path code EQ3/6. Mass balance calculations were conducted to estimate the extent of water-rock interaction between the intra-caldera tuffs and fluids. A mixing ratio of 82% thermal and 18% non-thermal water closely matches fluid compositions in Casa Diablo fluids as well as minerals observed in petrographic studies. Results of this study show that the mineralogy and fluid chemistry observed in the shallow reservoir at Long Valley caldera is formed by an open system of fluid-rock interaction. Further, calcite precipitated in the system serves as a sink for high levels of CO_2 generated by the deeper magmatic system. Our study shows that processes acting in a geothermal system can be effectively quantified using geochemical modeling and mass balance calculations.

References

Blackwell, D.D., 1985, A transient model of the geothermal system of the Long Valley caldera, California: Journal of Geophysical Research, v. 90, p. 11,229-11,241.

Farrar, C.D., M.L. Sorey, E. Roeloffs, D.L. Galloway, J.F. Howle, and R. Jacobson, 2003, Inferences on the hydrothermal system beneath the resurgent dome in Long Valley Caldera, east-central California, USA, from recent pumping tests and geochemical sampling: Journal of Volcanology and Geothermal Research, v. 127, p. 305-328.

Flexser, S., 1991, Hydrothermal alteration and past and present thermal regimes in the western moat of Long Valley caldera: Journal of Volcanology and Geothermal Research, v. 48, p. 303-318.

Hildreth, W., 2004, Volcanological perspective on Long Valley, Mammoth Mountain and Mono Craters: several contiguous but discrete systems: Journal of Volcanology and Geothermal Research, v. 136, p. 169-198.

McConnell, V.S., 1995, Hydrothermal history of the Long Valley Caldera, California: Life after collapse: Ph.D. thesis, University of Alaska, Fairbanks, Alaska, USA, 241 p.

McConnell, V.S., J.W. Valley, and J.C. Eichelberger, 1997, Oxygen isotope compositions of intra-caldera rocks: hydrothermal history of the Long Valley Caldera, California: Journal of Volcanology and Geothermal Research, v. 76, p. 83-109.

Pribnow, D.F.C., C. Schutze, S.J. Hurter, C. Flechsig, and J.H. Sass, 2003, Fluid flow in the resurgent dome of Long Valley Caldera: Implications from thermal data and deep electrical sounding: Journal of Volcanology and Geothermal Research, v. 127, p. 329-345.

Shevenell, L., F. Goff, C.O. Grigsby, C.J. Janik, P.E. Trujillo, and D. Counce, 1987, Chemical and isotopic characteristics of thermal fluids in the Long Valley Caldera lateral flow system, California: Transactions Geothermal Resources Council, v. 11, p. 195-201

Smith, B.M., and G.A. Suemnicht, 1991, Oxygen isotope evidence for past and present hydrothermal regimes of Long Valley caldera, California: Journal of Volcanology and Geothermal Research, v. 48, p. 319-339.

Sorey, M.L., 1985, Evolution and present state of the hydrothermal system in Long Valley caldera: Journal of Geophysical Research v. 90/B13, p. 11,219-11,228.

Sorey, M.L., G.A. Suemnicht, N.C. Sturchio, and G.A. Nordquist, 1991, New evidence on the hydrothermal system in Long Valley Caldera, California, from wells, fluid sampling, electrical geophysics, and age determinations of hot-spring deposits: Journal of Volcanology and Geothermal Research, v. 48, p. 229-263.

Tempel, R.N., and W.J. Harrison, 2000, Simulation of burial diagenesis in the Eocene Wilcox Group of the Gulf of Mexico basin: Applied Geochemistry, v. 15, p. 1071-1083.

Tempel, R.N., D.M. Sturmer, and J. Schilling, (in press), Geochemical modeling of the near-surface hydrothermal system beneath the southern moat of Long Valley Caldera, California: Geothermics.

White, A.F., and M.L. Peterson, 1991, Chemical equilibrium and mass balance relationships associated with the Long Valley hydrothermal system, California, USA: Journal of Volcanology and Geothermal Research, v. 48, p. 283-300.

Wolery, T.J., and S.A. Daveler, 1992, EQ3/EQ6, a software package for geochemical modeling of aqueous systems (version 7.0): Report UCRL-MA-110662 (1), Lawrence Livermore National Laboratory, Livermore, California, USA, 66 p.

Geochemical Modeling of the Near-Surface Hydrothermal System Beneath the Southern Moat of Long Valley Caldera, California

Regina Tempel and Daniel Sturmer
University of Nevada, Reno, Reno, NV, United States.

Abstract

Geochemical reaction path and mass balance modeling techniques were used to test the hypothesis that an eastwardly flowing plume of thermal water in the southern moat of the Long Valley caldera system reacts with hydrothermally-altered intra-caldera tuffs and mixes with non-thermal groundwater. Our conceptual model was based on hypotheses in the literature and utilized published geochemical and petrologic data. Mixing of thermal and non-thermal waters and reaction with wall rock was simulated using the reaction path code EQ3/6. Mass balance calculations were conducted to estimate the extent of water-rock interaction between the intra-caldera tuffs and fluids. A mixing ratio of 82% thermal and 18% non-thermal water closely matches fluid compositions in Casa Diablo fluids as well as minerals observed in petrographic studies. Results of this study show that the mineralogy and fluid chemistry observed in the shallow reservoir at Long Valley caldera is formed by fluid-rock interaction. Further, calcite precipitated in the system serves as a sink for high levels of CO_2 generated by the deeper magmatic system. Our study shows that processes acting in a geothermal system can be effectively quantified using geochemical modeling and mass balance calculations.

Introduction

A near-surface hydrothermal system within Long Valley caldera in east-central California possesses significant potential for geothermal energy development. Long Valley caldera is a resurgent caldera formed about 730,000 years ago, that has been studied extensively as a potential volcanic hazard because of renewed seismic activity and uplift within the resurgent dome beginning in 1980. As a result of the sustained volcanic activity, a shallow (<1 km), low temperature hydrothermal system exists in the southern part of Long Valley and extends from the West moat to the East moat of the caldera (Figure 1).
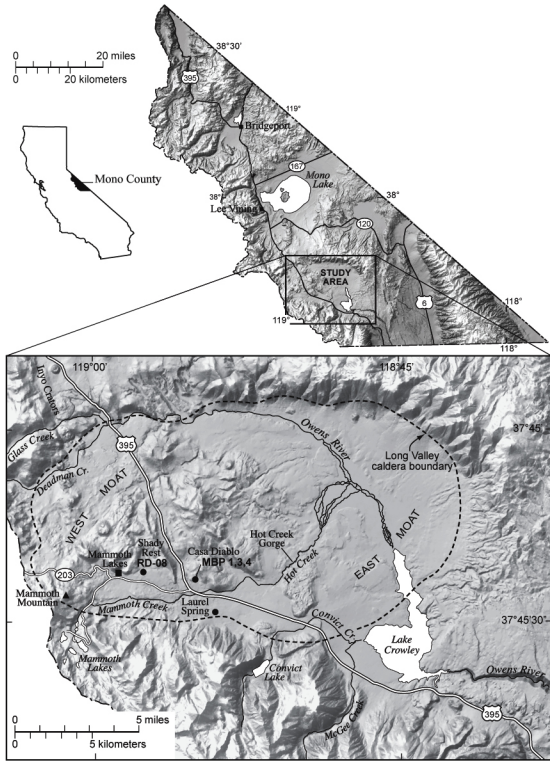

Figure 1. Map of the Long Valley caldera showing the location of selected wells and springs within the caldera.

Background

The current shallow hydrothermal system in Long Valley caldera has persisted for the past 40,000 years (Sorey et al., 1991; McConnell et al., 1997), while an earlier, deeper, higher temperature hydrothermal system peaked about 300,000 years ago (McConnell et al., 1997). The hydrothermal system is presumably driven by heat from intrusions during the last 200-300 ka beneath Mammoth Mountain (Smith and Suemnicht, 1991; Sorey et al., 1991; Farrar et al., 2003). The primary hydrothermal fluids in the active hydrothermal system rise up from a deep source reservoir in the basement rocks beneath the West Moat through faults and flow laterally to the southeast and discharge in the area around Hot Creek (Sorey et al., 1991; Farrar et al., 2003; Pribnow et al., 2003).

Thermal waters from hot springs have a temperature as high as 79-93°C, and become cooler in an easterly direction between Hot Creek and Lake Crowley (Figure 1) as the result of mixing between thermal water and shallow, cold groundwater and conductive cooling due to proximity with the land surface (Farrar et al., 2003; Shevenell et al., 1987; Sorey et al. 1991; Pribnow et al., 2003).
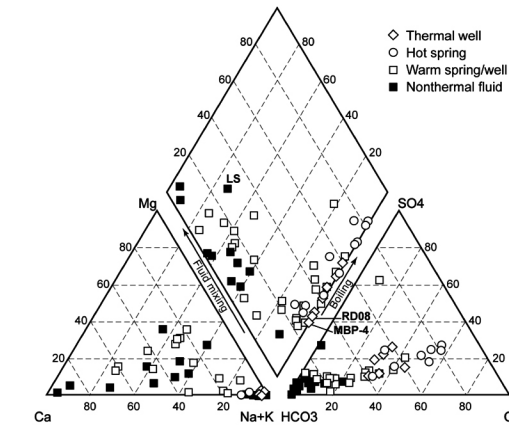

Figure 2. Piper diagram of major ion composition of water from springs and wells in the Long Valley Caldera.
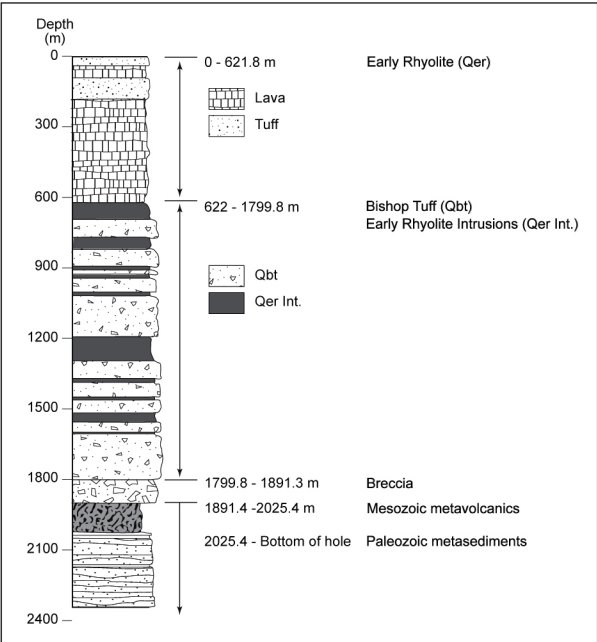

Figure 3. Stratigraphic relationships of major rock units in the Long Valley caldera as observed in the Long Valley Exploratory Well (LVEW) drilled into the resurgent dome (modified from McConnell et al., 1997).

Methods

We have developed a conceptual model to evaluate the hypothesis that the deep Long Valley hydrothermal fluid rises convectively in the western part of the caldera, reacts with the intracaldera tuffaceous units, and mixes with non-thermal groundwater to form an eastward laterally-flowing hydrothermal plume (Sorey, 1985; Blackwell, 1985) (Figure 4). The reaction path code, EQ3/6 (Wolery and Daveler, 1992), was utilized for this study. The modeling approach was based on the methods described by Tempel and Harrison (2000).
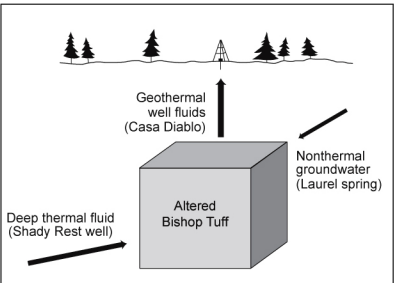

Figure 4. Schematic illustration of the conceptual model used to simulate the evolution of thermal fluids in the western part of the Long Valley hydrothermal system.

Table 1. Representative thermal and non-thermal fluid compositions from Long Valley caldera. Values given in mg/L. All well data from Farrar et al. (1989).

	Shady Rest well*	Casa Diablo well MBP-4	Laurel Spring
Sample date	11/13/86	7/14/86	4/10/86
Temperature (°C)	202	174	11.8
pH	5.9	6	8.6
Alkalinity (mg/L CaCO₃)	376	382	40
TDS	1430	1260	93
Ca	7.4	6.9	15
Mg	0.2	0.24	0.57
Na	369	350	5.8
K	43	36	1.2
SO4	159	110	15
Cl	280	230	0.4
F	12	10	0.05
SiO2	250	260	20
As	0.1	1.6	0.004
B	12	10	0.01
Li	2.8	--	0.005
Fe	35**	0.15	<0.003
Mn	0.29	0.038	<0.001

*Sample collected with bailer and analyzed by U.S. Geological Survey.
**Concentration of Fe is not representative of reservoir conditions, and is the result of fluid interaction with well casing.
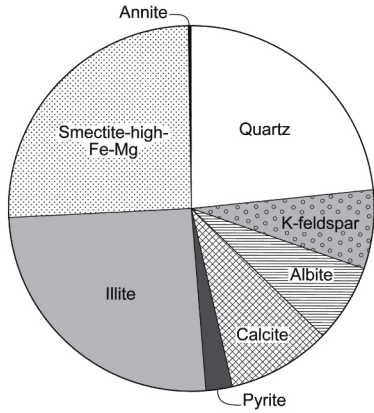

Figure 5. The reactants by volume used in modeling The altered intracaldera volcanic rocks.

Reactant mineral assemblages

Mineralogy of altered tuffs within the Bishop Tuff and Early Rhyolite was used to represent reactant mineral assemblages in all EQ3/6 reaction path calculations because it is volumetrically more significant than Early Rhyolite and compositionally similar (Hildreth, 2004). Minerals and their proportions were estimated from published petrographic and x-ray diffraction data (Flexser, 1991; McConnell, 1995) (Figure 5).

Table 2. Mass balance calculation with major ions used in estimating the amount of water-rock interaction between altered tuffs within the Bishop tuff and Early Rhyolite and formation fluids. Amounts are in mmol. Positive values are amounts dissolved or added to solution. Negative values are amounts removed from solution by precipitation or exsolution.

Amounts of reactants	Na	Ca	Mg	K	C	S	Cl	Si
0.82 Shady Rest fluid	13.16	0.15	0.007	0.90	22.1	1.36	6.50	3.40
0.18 Laurel Spring fluid	0.15	0.07	0.004	0.01	0.1	0.03	0.00	0.06
Calculated mixed water MBP-4 fluid	13.31	0.22	0.011	0.91	22.2	1.39	6.50	3.46
	15.20	0.17	0.010	0.92	27.5	1.15	6.50	4.30
Residual (Modeled mixed water minus MBP-4 fluid)	-1.89	0.05	0.001	-0.01	-5.3	0.24	0.00	-0.84
Dissolve 1.89 mmol albite	1.89							5.55
Dissolve 0.04 mmol anorthite and 0.01 mmol K-spar	0.00	0.05	0.001	-0.01	-5.3	0.24	0.00	4.71
	X	0.04						0.06
	X			0.01				0.03
Precipitate 0.004 mmol illite	0.00	0.09	0.001	0.000	-5.3	0.24	0.00	4.80
	X		-0.001	-0.01				-0.01
Dissolve 0.01 mmol K-spar	0.00	0.09	0.000	-0.01	-5.3	0.24	0.00	4.79
				0.01				0.03
Precipitate 0.83 mmol Ca-smectite	0.00	0.09	0.000	0.00	-5.3	0.24	0.00	4.82
	X	-0.14						-3.05
Precipitate 1.77 mmol quartz	0.00	-0.05	0.000	0.00	-5.3	0.24	0.00	1.77
	X							-1.77
Dissolve 0.05 mmol calcite	0.00	-0.05	0.000	0.00	-5.3	0.24	0.00	0.00
	X	0.05				0.05		
Dissolve 5.2 mmol CO2(g) and exsolve 0.24 mmol H2S(g)	0.00	0.00	0.000	0.00	5.2	0.24	0.00	0.00
	X					-0.24		
Totals	0.00	0.00	0.000	0.00	0.00	0.00	0.00	0.00

Table 3. Mineral percentages and volumes used to calculate the amounts of reactant minerals dissolved in the fluid over the course of the reaction path.

Mineral	Volumetric percentage	Molar volume (cc/mol)	Molar percentage	Mmol/L fluid
Quartz	23.3	22.688	14.69	27.2
K-feldspar	7.0	109.008	0.92	1.7
Albite	7.0	100.250	1.00	1.85
Anorthite*	--	--	--	0.05
Calcite	8.9	36.934	3.48	6.6
Pyrite	2.3	23.940	1.36	2.6
Illite	25.6	138.940	2.64	5.0
Smectite-high-Fe-Mg	25.6	139.070	2.64	5.0
Annite	0.2	154.320	0.02	0.035

*Anorthite was estimated by assuming a plagioclase composition of Ab₉₂An₀₂ (McConnel, 1995).

Table 4. Kinetic rates used in modeling mineral dissolution. Dissolution rate is given as mol/m²/s.

Mineral	Log dissolution rate	Relative rate	References
Albite	-12.26	1.0	Burch et al. (1993)
Illite[1]	-13.07	0.2	Knauss and Wolery (1986)
Quartz	-13.39	0.07	Rimstidt and Barnes (1980)
K-spar[2]	-12.50	0.06	
Smectite[3]		0.3	

[1]Rate for illite was assumed to be the same as that for muscovite (Lin and Clemency, 1981)
[2]Rate for K-spar was assumed to be the same as that listed for sanidine (Schweda, 1989).
[3]Rate for smectite was assumed to be similar to that for illite.

Results

In our study, a large number of reaction path calculations were performed in an attempt to model fluid mixing and reaction with altered tuffs within the Bishop Tuff and Early Rhyolite. Both open and closed system calculations were conducted to determine which calculation type represented the Long Valley system most closely. Results of our modeling calculations show that conservative mixing calculations closely match the fluid chemistry of the Casa Diablo wells, and that the open system water/rock calculations closely match the observed authigenic mineralogy of the Long Valley system.

Table 5. Calculated fluid redox values for three thermal wells in Long Valley caldera. Wells MBP-1 and MBP-3 are at the Casa Diablo geothermal plant. Modeled Eh and log fO_2 values are based on equilibrium with pyrite and reservoir conditions.

	MBP-1	MBP-3	Shady Rest
Temperature (°C)	168.0	171	202
Field pH	6.2	6.1	5.9
Modeled Eh	-0.26	-0.26	-0.25
Modeled log fO_2	-43	-42	-38

Table 6. Major aqueous species for each component in the MBP-1, MBP-3, and Shady Rest fluids. Each species is given as a percent of the total concentration.

		% OF TOTAL CONCENTRATION				
Component	Dominant Species	MBP-1	MBP-3	Shady Rest	Laurel	Mixed fluid
Al³⁺	AlO₂⁻	92	91	87	99	83
	HAlO₂(aq)	6	7	10	1	16
	NaAlO₂(aq)	2	2	3		1
B(OH)₃(aq)	B(OH)₃(aq)	100	100	100	85	100
	BO₂⁻				14	
Ca²⁺	Ca²⁺	69	70	52	97	70
	CaHCO₃⁺	5	4	3		2
	CaSO₄(aq)	24	23	42	1	26
Cl⁻	Cl⁻	99	99	99	100	99
F⁻	F⁻	97	97	91	98	94
	HF(aq)	2	2	7		5
Fe²⁺	Fe²⁺	97	96	93		97
	FeCl⁺	3	4	7		3
	Fe(OH)₂(aq)				90	
	Fe(OH)₃⁻				9	
H₂AsO₄⁻	HAsO₄(aq)	85	86	93		85
	H₂AsO₄(aq)	15	14	7		15
	AsO₄²⁻				100	
HCO₃⁻	CO₂(aq)	80	84	94	1	92
	HCO₃⁻	20	16	6	97	8
K⁺	K⁺	97	97	95	100	97
Li⁺	Li⁺	100	100	100	100	100
Mg²⁺	MgSO₄(aq)	86	86	96	2	87
	Mg²⁺	12	12	3	97	11
Na⁺	Na⁺	99	99	99	100	99
SO₄²⁻	SO₄²⁻	92	89	88	97	91
	HS⁻	3	6	2		1
	H₂S(aq)	1	5	2		2
SiO₂(aq)	SiO₂(aq)	100	100	100	100	100

Table 7. Results of single-point reaction path calculations showing mass of product phases in milligrams precipitated from one liter of reservoir fluid. Products are listed for two sets of calculations, one in which no mineral phases were suppressed and one in which talc, dolomite, diaspore, corundum, and boehmite were suppressed.

	MILLIGRAMS PRECIPITATED				
Dominant Species	MBP-1	MBP-3	Shady Rest	Laurel	Mixed fluid
No mineral phases suppressed:					
Quartz	116.48	110.60	19.850	16.410	69.79
Talc					
Pyrite	0.80	1.74	0.099		0.10
Calcite				0.067	
Hematite				0.004	
Minerals suppressed:					
Quartz	116.48	110.60	19.850	16.410	69.79
Pyrite	0.80	1.74	0.099		0.10
Calcite				0.067	
Hematite				0.004	

Table 8. Comparison of fluid characteristics between Casa Diablo well fluids and modeled fluids. Fluid data from Farrar et al. (1989). Concentrations in mg/L.

	MBP-1	MBP-3	MBP-4	Modeled mixed waters	Open model water/rock	Closed model water/rock
Temperature (°C)	168	171	174	168	168	168
pH	6.2	6.1	6.0	5.7	6.4	6.4
Eh (calc.)	-0.25	-0.25	-0.25	-0.21	-0.28	-0.28
Al	n.a.	n.a	n.a	n.a.	0.04	0.04
B	11	10	11	10	10	10
Ca	2.6	2.5	6.9	8.6	20	20
Cl	260	250	230	227	227	227
F	12	11	10	10	10	10
Fe	0.38	0.83	0.15	0.009	0.00005	0.00005
As	1.1	0.72	1.6	0.06	0.06	0.06
HCO₃	438*	422*	466*	376	448	453
K	34	33	36	35	47	50
Li	2.7	2.8	n.a.	2.2	2.2	2.2
Mg	0.64	0.55	0.24	0.26	0.58	0.59
Na	370	360	350	297	310	310
SO₄	130	120	110	130	125	125
SiO₂	270	270	260	204	147	147

*Calculated from alkalinity as calcium carbonate

Reactant mineral assemblages

Mineralogy of altered tuffs within the Bishop Tuff and Early Rhyolite was used to represent reactant mineral assemblages in all EQ3/6 reaction path calculations, because it is volumetrically more significant than Early Rhyolite and compositionally similar (Hildreth, 2004). Minerals and their proportions were estimated from published petrographic and x-ray diffraction data (Flexser, 1991; McConnell, 1995) (Figure 5).
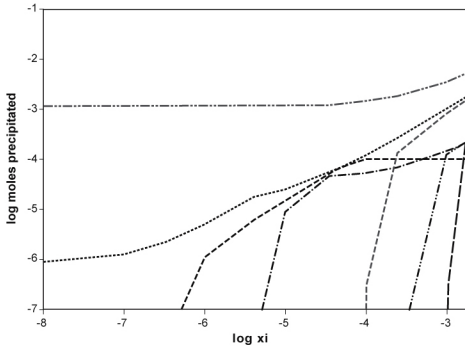

Figure 6. Product mineralogy resulting from modeling of mixing and water-rock interaction in open system conditions. Log xi horizontal axis represents reaction progress.
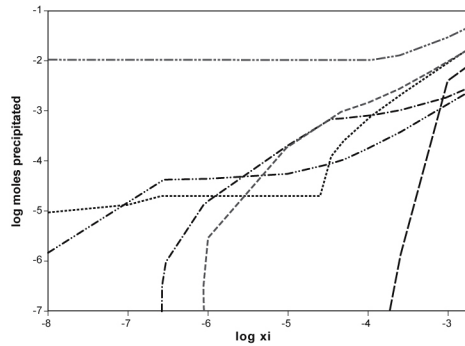

Figure 7. Product mineralogy resulting from fixed-fugacity of log P_{CO_2} of -2.3 (5.3 mmol/L) in an open system calculation. Log xi on horizontal axis represents reaction progress.

Conclusions

Our findings that: (1) the open system model best represents the observed secondary mineral assemblage within the Long Valley caldera, (2) conservative mixing of 82% Shady Rest and 18% Laurel Spring waters matches Casa Diablo well chemistry, and (3) the fluid phase appears to be an important source for quartz, pyrite, smectite, and hematite, are consistent with previous studies that have found that flow rates in the Long Valley system are high (100-200 m/yr) and indicative of an open system (i.e. Blackwell, 1985). The resultant water chemistry from water-rock interaction calculations is not considerably different than the conservative mixing model water chemistry and does not vary similar to the actual water compositions at Casa Diablo (Table 8). This observation suggests that dissolution of feldspars, the dominant reactive mineral phase, results in minimal formation of clay minerals and calcite in the reservoir.

Acknowledgements

References

Blackwell, D.D., 1985. A transient model of the geothermal system of the Long Valley caldera, California. Journal of Geophysical Research 90, 11,229-11,241.

Farrar, C.D., Sorey, M.L., Roeloffs, E., Galloway, D.L., Howle, J.F., Jacobson, R., 2003. Inferences on the hydrothermal system beneath the resurgent dome in Long Valley Caldera, east-central California, USA, from recent pumping tests and geochemical sampling. Journal of Volcanology and Geothermal Research 127, 305-328.

Flexser, S., 1991. Hydrothermal alteration and past and present thermal regimes in the western moat of Long Valley caldera. Journal of Volcanology and Geothermal Research 48, 303-318.

Hildreth, W., 2004. Volcanological perspective on Long Valley, Mammoth Mountain and Mono Craters: several contiguous but discrete systems. Journal of Volcanology and Geothermal Research 136, 169-198.

McConnell, V.S., 1995. Hydrothermal history of the Long Valley Caldera, California: Life after collapse. Ph.D. thesis. University of Alaska, Fairbanks, AK, USA, 241 pp.

McConnell, V.S., Valley, J.W., Eichelberger, J.C., 1997. Oxygen isotope compositions of intra-caldera rocks: hydrothermal history of the Long Valley Caldera, California. Journal of Volcanology and Geothermal Research 76, 83-109.

Pribnow, D.F.C., Schutze, C., Hurter, S.J., Flechsig, C., Sass, J.H., 2003. Fluid flow in the resurgent dome of Long Valley Caldera: Implications from thermal data and deep electrical sounding. Journal of Volcanology and Geothermal Research 127, 329-345.

Shevenell, L., Goff, F., Grigsby, C.O., Janik, C.J., Trujillo, P.E., Counce, D., 1987. Chemical and isotopic characteristics of thermal fluids in the Long Valley Caldera lateral flow system, California. Transactions Geothermal Resources Council 11, 195-201.

Smith, B.M., Suemnicht, G.A., 1991. Oxygen isotope evidence for past and present hydrothermal regimes of Long Valley caldera, California. Journal of Volcanology and Geothermal Research 48, 319-339.

Sorey, M.L., 1985. Evolution and present state of the hydrothermal system of the Long Valley caldera, California. Journal of Geophysical Research 90(B13), 11,219-11,228.

Sorey, M.L., Suemnicht, G.A., Sturchio, N.C., Nordquist, G.A., 1991. New evidence on the hydrothermal system in Long Valley Caldera, California, from wells, fluid sampling, electrical geophysics, and age determinations of hot-spring deposits. Journal of Volcanology and Geothermal Research 48, 229-263.

Tempel, R.N., Harrison, W.J., 2000. Simulation of burial diagenesis in the Eocene Wilcox Group of the Gulf of Mexico basin. Applied Geochemistry 15, 1071-1083.

Tempel, R.N., Sturmer, D.M., Schilling, J., 2011, Geochemical modeling of the near-surface hydrothermal system beneath the southern moat of Long Valley Caldera, California. Geochemics, (in press).

White, A.F., Peterson, M.L., 1991. Chemical equilibrium and mass balance relationships associated with the Long Valley hydrothermal system, California, U.S.A. Journal of Volcanology and Geothermal Research 48, 283-300.

Wolery, T.J., Daveler, S.A., 1992. EQ3/EQ6, a software package for geochemical modeling of aqueous systems (version 7.0). Report UCRL-MA-110662 (1), Lawrence Livermore National Laboratory, Livermore, CA, USA, 66 pp.